

Rate-Splitting Multiple Access for Multi-antenna Downlink Communication Systems: Spectral and Energy Efficiency Tradeoff

Gui Zhou, Yijie Mao, Bruno Clerckx, *Senior Member, IEEE*

Abstract—Rate-splitting (RS) has recently been recognized as a promising physical-layer technique for multi-antenna broadcast channels (BC). Due to its ability to partially decode the interference and partially treat the remaining interference as noise, RS is an enabler for a powerful multiple access, namely rate-splitting multiple access (RSMA), that has been shown to achieve higher spectral efficiency (SE) and energy efficiency (EE) than both space division multiple access (SDMA) and non-orthogonal multiple access (NOMA) in a wide range of user deployments and network loads. As SE maximization and EE maximization are two conflicting objectives, the study of the tradeoff between the two criteria is of particular interest. In this work, we address the SE-EE tradeoff by studying the joint SE and EE maximization problem of RSMA in multiple input single output (MISO) BC with rate-dependent circuit power consumption at the transmitter. To tackle the challenges coming from multiple objective functions and rate-dependent circuit power consumption, we first propose two methods to transform the original problem into a single-objective problem, namely, weighted-sum method and weighted-power method. A successive convex approximation (SCA)-based algorithm is then proposed to jointly optimize the precoders and RS message split of the transformed problem. Numerical results show that our algorithm converges much faster than existing algorithms. In addition, the performance of RS is superior to or equal to non-RS strategy in terms of both SE and EE and their tradeoff.

Index Terms—Rate-splitting, spectral efficiency, energy efficiency, precoder design, successive convex approximation (SCA).

I. INTRODUCTION

Rate-splitting (RS) has recently emerged in multi-antenna broadcast channel (BC) as a powerful and robust non-orthogonal transmission technique and interference management strategy for cellular networks. At the base station (BS), the message intended for each user is split into a common and a private part. After jointly encoding the common parts into a common stream to be decoded by all users and independently encoding the private parts into the private streams for the corresponding users only, BS linearly precodes all the encoded streams and broadcasts the superimposed data streams to all users. By allowing each user to sequentially decode the common stream and

G. Zhou is with the School of Electronic Engineering and Computer Science at Queen Mary University of London, London E1 4NS, U.K. (e-mail: g.zhou@qmul.ac.uk). B. Clerckx and Y. Mao are with the Electrical and Electronic Engineering Department, Imperial College London, London SW7 2AZ, U.K. (e-mail: b.clerckx, y.mao16@imperial.ac.uk).

the intended private stream with the assistance of successive interference cancellation (SIC), RS grants all users the ability to partially decode the interference and partially treat the remaining interference as noise.

The study of RS dates back to early 1980s in [1] for the two-user single-input single-output (SISO) interference channel (IC). The flexibility of RS in dealing with interference in SISO IC has motivated the investigation of the benefits of RS in modern multiple input single output (MISO) BC [2], [3]. As the two fundamental indicators for a communication system design, spectral efficiency (SE) demonstrates the amount of information to be transmitted per unit of time while energy efficiency (EE) demonstrates how much information rate can be transmitted per unit of energy. Existing literature of RS in MISO BC has shown that RS is an enabler for a powerful multiple access, namely rate-splitting multiple access (RSMA), that achieves both higher SE and EE over space division multiple access (SDMA) and non-orthogonal multiple access (NOMA) in both perfect Channel State Information at the Transmitter (CSIT) [4]–[8] and imperfect CSIT [9]–[14]. Compared with RSMA that dynamically partially decodes the interference and partially treats interference as noise, SDMA and NOMA fall into two extreme interference management cases where users in SDMA always decode their intended signal by fully treating any residual interference as noise and users in NOMA always fully decode the interference generated by the users with weaker channel strengths [5]. Besides conventional MISO BC, the benefits of RS in the SE domain have been further demonstrated in massive MISO system [10], millimeter wave system [11], overloaded system [14], MISO BC with user relaying [15], etc. The benefits of RS from an EE perspective are also investigated in MISO BC [16], and MISO BC with a common message (so-called non-orthogonal unicast and multicast transmission) [4].

However, since EE is a quasi-convex function with respect to transmit signal-to-noise (SNR) and SE is a monotonic-increasing function of SNR, EE and SE conflict with each other in the high SNR regime [17]. This conflict leads to a fundamental tradeoff between SE and EE, which needs to be studied so as to provide guidance for system designers on how to balance the two metrics.

The SE-EE tradeoff optimization problem is a multi-objective optimization (MOO) problem which is generally

transformed to its corresponding single-objective optimization (SOO) problems such as weighted sum method [18], [19], epsilon-constraint method [20], etc. Two widely used precoder design frameworks to solve the transformed SOO problems are Dinkelbach's framework [21] [22] and successive convex approximation (SCA) framework [23] [24] or called inner approximation (IA) framework [25]. The key step of the Dinkelbach's framework is to transform the fractional program into a sequence of parametric problems by introducing an auxiliary variable, which can then be solved by zero forcing (ZF) [26], weighted minimum mean square error (WMMSE) [27], SCA methods [28], monotonic optimization [29], [30]. It is indeed a two-layer iterative algorithm framework, which optimizes the parameter in the outer layer and precoder in the inner layer. In comparison, SCA framework can be directly applied to solve the SE-EE tradeoff problem by approximating the fractional EE metric as well as other non-convex expressions into their convex approximation counterparts, which results in a one-layer iterative algorithm. The SCA framework has shown its performance advantages in terms of convergence compared to the Dinkelbach's framework in conventional communication systems with orthogonal multiple access (OMA) [24].

In this work, we investigate the SE-EE tradeoff of RSMA in multi-user multi-antenna systems. The major contributions of this work are as follows:

- We investigate the SE-EE tradeoff achieved by RSMA in a MISO BC. Previous works on RS either address the SE (as in [4]–[7], [9]–[14]) or EE (as in [4], [16]), but the tradeoff between SE and EE has never been studied. It should be reminded that, since RSMA is a general framework for non-orthogonal transmission that subsumes SDMA, NOMA, OMA and multicasting as special cases [3], [5], identifying the SE-EE tradeoff of RSMA automatically solves the SE-EE tradeoff of those particular strategies.
- We formulate a MOO problem that jointly maximizes SE and EE of RSMA in a MISO BC subject to an average transmit power constraint. To obtain reasonable operating points on the Pareto boundary that balance SE and EE, we adopt two different approaches to convert the MOO problem into a SOO problem, namely the weighted-sum and the weighted-power approaches. The former transformation is achieved by maximizing the weighted sum of SE and EE and the latter is to minimize the weighted sum of the inverse of both SE and EE.
- Due to the non-convexity of the transformed SOO problems, we propose a SCA-based framework to solve both weighted-sum and weighted-power problems with two different rate lower bounds to relax the non-convex rate constraints, namely “LB I” and “LB II”. LB I is achieved by exploiting the convexity of log function and directly using the first-order Taylor approximation of the rate function. In comparison, LB II is obtained by approximating the fractional signal-to-interference

plus-noise ratio (SINR) expression only. The proposed SCA-based algorithm is shown to not only solve the SE-EE tradeoff problem but also the individual SE and EE problems.

- We demonstrate through numerical results that RS achieves a larger achievable SE and EE tradeoff region than the conventional multi-user linearly-precoded Non-RS (NoRS) strategy (commonly used in SDMA and multi-user MIMO) in different user deployments, SE and EE weights, transmit power constraints, etc. We further evaluate the convergence and complexity of the developed algorithm by observing the CPU time and the number of required iterations. The proposed SCA-based algorithm with both lower bound LB I and II converges within a few iterations and is faster than the existing Dinkelbach's algorithm. LB I converges slightly slower than LB II but both converge to similar boundary point. We conclude that RS can not only improve individual SE and EE, but also achieve a better SE-EE tradeoff in multi-antenna BC.

The remaining of this paper is organized as follows. In Section II, the system model is specified and the optimization problems are formulated. The weighted-sum approach is proposed to design the precoder in Section III. A weighted-power approach is proposed to design the precoder in Section IV. Section V and Section VI show the numerical results and conclusion, respectively.

Notations: Vectors and matrices are denoted by boldface lowercase and uppercase letters, respectively. The symbols \mathbf{x}^* , \mathbf{x}^T and \mathbf{x}^H denote the conjugate, transpose, and Hermitian (conjugate transpose) of vector \mathbf{x} , respectively. Additionally, the symbol \mathbb{C} denotes complex field and \mathbb{R} represents real field. The symbol $\|\mathbf{x}\|_2$ denotes 2-norm of vector \mathbf{x} and the symbol $\|\mathbf{X}\|_F$ denotes Frobenius norm of matrix \mathbf{X} . The symbols $\text{Tr}\{\cdot\}$, $\text{Re}\{\cdot\}$, and $|\cdot|$ denote the trace, real part and modulus, respectively.

II. SYSTEM MODEL AND PROBLEM FORMULATION

In this section, we specify the system model of RS in MISO BC followed by the formulated SE and EE tradeoff problem. The rate-dependent power consumption model of the transmitter is also specified in this section.

A. Rate-Splitting Transmit Signal Model

In this work, we consider a downlink multi-antenna multi-user communication system where one base station (BS) with N_t transmit antennas transmits K messages simultaneously to K single-antenna users. The principle of RS strategy is discussed as follows. At the BS, the message W_k intended for user k is split into a private part $W_{p,k}$ and a common part $W_{c,k}$. The private parts $W_{p,1}, \dots, W_{p,K}$ are independently encoded into the private streams s_1, \dots, s_K and the common parts of all users $W_{c,1}, \dots, W_{c,K}$ are combined into a common message W_c , which is encoded into a common stream s_c using a public codebook. Denoting $\mathbf{s} = [s_c, s_1, \dots, s_K]^T$ and assuming Gaussian signaling with

$\mathbb{E}[\mathbf{ss}^H] = \mathbf{I}$, the $K + 1$ streams are linearly precoded by precoding vectors $\mathbf{f}_c, \mathbf{f}_1, \dots, \mathbf{f}_K$. Define set $\mathcal{K}_c = \mathcal{K} \cup \{c\}$ and set $\mathcal{K} = \{1, 2, \dots, K\}$, the resulting transmit signal of RS strategy can be written as

$$\mathbf{x} = \sum_{i \in \mathcal{K}_c} \mathbf{f}_i s_i. \quad (1)$$

We use a compact notation \mathbf{F} to denote the family of the precoder vectors as $\mathbf{F} = [\mathbf{f}_c, \mathbf{f}_1, \dots, \mathbf{f}_K] \in \mathbb{C}^{N_t \times (K+1)}$. It belongs to the power constraint set $\mathcal{S} = \{\mathbf{F} \mid \|\mathbf{F}\|_F^2 \leq P_{\max}\}$ where P_{\max} is the maximum available transmit power at the BS.

The received signal of user k is

$$y_k = \mathbf{h}_k^H \sum_{i \in \mathcal{K}_c} \mathbf{f}_i s_i + n_k, \quad (2)$$

where $\mathbf{h}_k \in \mathbb{C}^{N_t \times 1}$ is the channel between BS and user k and noise n_k follows Gaussian distribution, i.e., $\mathcal{N}(0, \sigma_k^2)$. In this work, we assume perfect CSIT.

At the receivers, each user firstly decodes the common stream by treating all the private streams as noise, then SIC is used to remove the decoded common stream from the received signal under the assumption of error-free decoding. Each user then decodes its own private stream by treating other private streams as noise. Thus, the spectral efficiencies (bit/s/Hz) of the intended common and private streams at user k are formulated as

$$R_{c,k}(\mathbf{F}) = \log_2 \left(1 + \frac{\mathbf{h}_k^H \mathbf{f}_c \mathbf{f}_c^H \mathbf{h}_k}{\sigma_k^2 + \sum_{i \in \mathcal{K}} \mathbf{h}_k^H \mathbf{f}_i \mathbf{f}_i^H \mathbf{h}_k} \right), \quad (3)$$

$$R_k(\mathbf{F}) = \log_2 \left(1 + \frac{\mathbf{h}_k^H \mathbf{f}_k \mathbf{f}_k^H \mathbf{h}_k}{\sigma_k^2 + \sum_{i \in \mathcal{K} \setminus \{k\}} \mathbf{h}_k^H \mathbf{f}_i \mathbf{f}_i^H \mathbf{h}_k} \right). \quad (4)$$

The achievable SE of the common stream is given as $R_c(\mathbf{F}) = \min_{k \in \mathcal{K}} R_{c,k}(\mathbf{F})$ in order to guarantee that all users are capable of decoding the common stream successfully. Therefore, the system SE is the sum of the SE of the common and private streams, which is given by

$$f(\mathbf{F}) = \sum_{k \in \mathcal{K}_c} R_k(\mathbf{F}). \quad (5)$$

B. Spectral Efficiency Maximization

The existing literature [5], [10]–[15] have investigated precoder design of RS for maximizing the SE in various scenarios. The SE maximization problem is formulated as follows

$$\max_{\mathbf{F} \in \mathcal{S}} f(\mathbf{F}). \quad (6)$$

Popular precoding techniques rely on closed form precoders based on ZF method [26] for private messages as in [3], [9]–[11], or optimized precoders based on convex optimization commonly relying on an extended version of the WMMSE method [27], as in [5], [12]–[15]).

C. Energy Efficiency Maximization

As another important performance metric, EE benefits of RS strategy in multi-antenna BC have only been studied in a few literature [4], [16] and only constant circuit power consumption is considered in those works. However, in practical communication systems, the circuit power consumption contains two parts, namely the rate-independent fixed part and the rate-dependent dynamic part [31], [32]. The former is for basic circuit operations, e.g., channel estimation, precoder chains, and linear processing at the BS while the latter is for information processing, e.g., coding, decoding and backhaul power consumption. In this work, we consider a more practical power consumption model that has not been studied in the literature of RS yet. We adopt the power consumption model of [32], [33], where the rate-dependent circuit power consumption is written as a linear function of the system sum-rate. Therefore, the total power consumption is modeled as

$$g(\mathbf{F}) = \|\mathbf{F}\|_F^2 + P_c + \chi f(\mathbf{F}), \quad (7)$$

where $\|\mathbf{F}\|_F^2$ is the transmit power consumption, P_c is a constant representing the rate-independent fixed power consumption, and $\chi \geq 0$ is a constant demonstrating the coding, decoding, and backhaul power consumption per unit data rate (W/(bit/s/Hz)) [31].

The corresponding EE maximization problem under the practical power consumption model is formulated as

$$\max_{\mathbf{F} \in \mathcal{S}} \frac{f(\mathbf{F})}{g(\mathbf{F})}. \quad (8)$$

Problem (8) is a fractional programming with non-concave numerator and non-convex denominator, which is hard to be solved directly. In addition, the non-convex practical power consumption model with non-linear rate expression makes the entire problem more complex to solve.

D. Spectral Efficiency and Energy Efficiency Tradeoff

The system SE is an increasing function of the transmit power consumption and its maximization is achieved by consuming all available transmit power. Such a strategy may not be suitable for EE maximization, since EE tries to balance SE and power consumption. Hence, EE and SE are two conflicting metrics, which results in a SE-EE tradeoff. The goal is to characterize this tradeoff and identify the precoder strategy that achieves the best SE-EE tradeoff. The SE-EE tradeoff is a MOO problem, which is given by

$$\max_{\mathbf{F} \in \mathcal{S}} \left[\frac{f(\mathbf{F})}{g(\mathbf{F})}, f(\mathbf{F}) \right]. \quad (9)$$

The solutions of Problem (9) are Pareto optimal since none of the objective value can be improved without reducing that of the other.

There are several methods to find the Pareto optimal solutions of a multi-objective problem. The first one is weighted sum method [18], [19], which collapses the multiple objectives into a single objective by summing up all

the objective functions with a specific weight given to each objective function. Another one is epsilon-constraint method [4], [20], in where one of the original objectives is maximized under the new constraints transformed from the other objectives.

To solve the MOO Problem (9), we adopt two different methods to obtain the Pareto optimal solutions, namely, the weighted-sum approach and the weighted power approach. The two approaches will be specified in the following Section III and IV, respectively.

Note that the SE maximization Problem (6) and the EE maximization Problem (8) are actually special cases of the SE-EE tradeoff Problem (9). As a consequence, individual problems (6) and (8) can also be solved under the framework of our proposed algorithm for Problem (9).

III. WEIGHDED-SUM APPROACH

In this section, the weighted-sum approach to solve Problem (9) is specified. Weighted-sum approach is a classical method to solve MOO. It converts MOO into a SOO problem by assigning a weight to each normalized objective function and sum them up. Therefore, the MOO of (9) is transformed into

$$\max_{\mathbf{F} \in \mathcal{S}} w \frac{f(\mathbf{F})}{g(\mathbf{F})} + (1-w) \frac{f(\mathbf{F})}{P_c}, \quad (10)$$

where $w \in [0, 1]$ is a constant to control the priority of EE and SE. As in [19], the denominator P_c of the second fraction in (10) is introduced to unify the units of the two objective functions in (9) so that the values are comparable. We remark that the denominator of the second term is a constant which could be chosen randomly without affecting the solutions of Problem (10).

Problem (10) is difficult to solve for the reason that the objective function has non-convex numerator and denominator, and the non-convex property mainly comes from the rate expressions. A popular method to solve general fractional programming problem is Dinkelbach's method [21]. It is capable of converting fractional programming to linear programming by introducing parameters to denote those fractions. These parametric linear programming problems are then addressed by applying SCA [34] and WMMSE [22]. The Dinkelbach's framework is in fact a two-layer iterative procedure, which requires huge computational complexity. More importantly, the convergence of this framework cannot be guaranteed since each parametric linear programming problem may only achieve local optimum [24].

A. SCA-based Algorithm

In order to address the above shortcomings, we propose a one-layer iterative algorithm under the SCA framework [23] directly. Firstly, we introduce a new variable η denoting the EE and reformulate Problem (10) as

$$\max_{\mathbf{F} \in \mathcal{S}, \eta} w\eta + (1-w) \frac{f(\mathbf{F})}{P_c} \quad (11a)$$

$$\text{s.t. } \eta \leq \frac{f(\mathbf{F})}{g(\mathbf{F})}. \quad (11b)$$

To tractably recast non-convex fractional constraint (11b), we replace it with the following three constraints

$$\eta \leq \frac{x^2}{y}, \quad (12a)$$

$$x^2 \leq f(\mathbf{F}), \quad (12b)$$

$$g(\mathbf{F}) \leq y, \quad (12c)$$

where variable x represents the square root of the total sum rate, and variable y represents the total power. Then, we introduce variables $\mathbf{r} = [r_c, r_1, \dots, r_K]^T$ to denote rates $\{R_i(\mathbf{F})\}_{i \in \mathcal{K}_c}$ and rewrite Problem (11) equivalently as

$$\max_{\mathbf{F} \in \mathcal{S}, \eta, \mathbf{r}, x, y} w\eta + \frac{(1-w)}{P_c} \sum_{i \in \mathcal{K}_c} r_i \quad (13a)$$

$$\text{s.t. } (12a)$$

$$x^2 \leq \sum_{i \in \mathcal{K}_c} r_i \quad (13b)$$

$$\|\mathbf{F}\|_F^2 + P_c + \chi \sum_{i \in \mathcal{K}_c} r_i \leq y \quad (13c)$$

$$r_k \leq R_k(\mathbf{F}), \forall k \in \mathcal{K} \quad (13d)$$

$$r_c \leq R_{c,k}(\mathbf{F}), \forall k \in \mathcal{K} \quad (13e)$$

The non-convexity of Problem (13a) is due to the constraints (12a), (13d) and (13e), which motivates us to use SCA framework to approximate the non-convex constraints. Specifically the right hand side of (12a) is a quadratic-over-linear function, which is jointly convex in (x, y) . We approximate it by its first-order lower approximation at fixed point $(x^{(n)}, y^{(n)})$ as [35]

$$\frac{x^2}{y} \geq \frac{2x^{(n)}}{y^{(n)}}x - \left(\frac{x^{(n)}}{y^{(n)}} \right)^2 y \triangleq \phi^{(n)}(x, y). \quad (14)$$

The remaining challenge is to tackle the non-convexity of constraints (13d) and (13e). In most literature, the relation between rate and WMMSE is used to transform the non-convex rate-based function into its convex WMMSE counterpart by introducing auxiliary variables, i.e., weights and equalizers. The method known as WMMSE is widely used in the literature [13], [22], [23] and shows good performance. However, WMMSE method is an iterative optimization method, in which the weights, equalizers and precoders are updated in an iterative manner.

In the following, we investigate the intrinsic convexity of the rate expressions $R_k(\mathbf{F})$ and $R_{c,k}(\mathbf{F})$, and then propose two lower bounds of approximating the non-convex rate expressions.

1) *Lower-bound (LB) I*: The first lower bound of rate is summarized in the following Lemma 1.

Lemma 1 *Let $\mathbf{F}^{(n)}$ denote the optimal solution obtained in the $(n-1)$ -th iteration. The concave lower bound function of $R_k(\mathbf{F})$ in the n -th iteration is given by*

$$R_k^{(n)}(\mathbf{F}) \triangleq \text{const}_k + 2\text{Re} \left\{ a_k \mathbf{b}_k^H \mathbf{f}_k \right\} - a_k \sum_{i \in \mathcal{K}} \mathbf{f}_i^H \mathbf{b}_k \mathbf{b}_k^H \mathbf{f}_i, \quad (15)$$

at point $\mathbf{F}^{(n)}$, where

$$a_k = 1 + (\sigma_k^2 + \sum_{i \in \mathcal{K} \setminus \{k\}} \mathbf{h}_k^H \mathbf{f}_i^{(n),H} \mathbf{h}_k)^{-1} \mathbf{f}_k^{(n),H} \mathbf{h}_k \mathbf{h}_k^H \mathbf{f}_k^{(n)}, \quad (16)$$

$$\mathbf{b}_k = (\sigma_k^2 + \sum_{i \in \mathcal{K}} \mathbf{h}_k^H \mathbf{f}_i^{(n),H} \mathbf{h}_k)^{-1} \mathbf{h}_k^H \mathbf{f}_k^{(n)} \mathbf{h}_k, \quad (17)$$

$$\begin{aligned} \text{const}_k &= R_k \left(\mathbf{F}^{(n)} \right) - 2\text{Re} \left\{ a_k \mathbf{b}_k^H \mathbf{f}_k^{(n)} \right\} \\ &\quad + a_k \sum_{i \in \mathcal{K}} \mathbf{f}_i^{(n),H} \mathbf{b}_k \mathbf{b}_k^H \mathbf{f}_i^{(n)}. \end{aligned} \quad (18)$$

Meanwhile, the concave lower bound function of $R_{c,k}(\mathbf{F})$ is given by

$$\begin{aligned} R_{c,k}^{(n)}(\mathbf{F}) &\triangleq \\ \text{const}_{c,k} &+ 2\text{Re} \left\{ a_{c,k} \mathbf{b}_{c,k}^H \mathbf{f}_c \right\} - a_{c,k} \sum_{i \in \mathcal{K}_c} \mathbf{f}_i^H \mathbf{b}_{c,k} \mathbf{b}_{c,k}^H \mathbf{f}_i, \end{aligned} \quad (19)$$

at point \mathbf{f}^n , where

$$a_{c,k} = 1 + (\sigma_k^2 + \sum_{i \in \mathcal{K}} \mathbf{h}_k^H \mathbf{f}_i^{(n),H} \mathbf{h}_k)^{-1} \mathbf{f}_c^{(n),H} \mathbf{h}_k \mathbf{h}_k^H \mathbf{f}_c^{(n)}, \quad (20)$$

$$\mathbf{b}_{c,k} = (\sigma_k^2 + \sum_{i \in \mathcal{K}_c} \mathbf{h}_k^H \mathbf{f}_i^{(n),H} \mathbf{h}_k)^{-1} \mathbf{h}_k^H \mathbf{f}_c^{(n)} \mathbf{h}_k, \quad (21)$$

$$\begin{aligned} \text{const}_{c,k} &= R_{c,k} \left(\mathbf{F}^{(n)} \right) - 2\text{Re} \left\{ a_{c,k} \mathbf{b}_{c,k}^H \mathbf{f}_c^{(n)} \right\} \\ &\quad + a_{c,k} \sum_{i \in \mathcal{K}_c} \mathbf{f}_i^{(n),H} \mathbf{b}_{c,k} \mathbf{b}_{c,k}^H \mathbf{f}_i^{(n)}. \end{aligned} \quad (22)$$

Proof: Please refer to Appendix A. \blacksquare

As we mentioned before, many works address the non-convex problem with rate-based utility function by using the relation between rate and WMMSE. Actually, the following Lemma reveals the connection between the lower bound of rate in Lemma 1 and that derived via WMMSE.

Lemma 2 In perfect CSIT, our proposed lower bounds of rate in Lemma 1 is the same with the WMMSE-based lower bound [36].

Proof: Please refer to Appendix A. \blacksquare

Recall that the WMMSE method is based on an alternating optimization framework. While, by adopting the proposed LB I, the optimal solutions of all variables can be found in each iteration, which provides better fixed point for the next iteration.

With the concave lower bound approximations (14), (19), and (20), Problem (13) is reformulated equivalently as the following convex problem:

$$\max_{\mathbf{F} \in \mathcal{S}, \eta, \mathbf{r}, x, y} w\eta + \frac{(1-w)}{P_c} \sum_{i \in \mathcal{K}_c} r_i \quad (23a)$$

$$\text{s.t. } \eta \leq \phi^{(n)}(x, y) \quad (23b)$$

$$r_k \leq R_k^{(n)}, \forall k \in \mathcal{K} \quad (23c)$$

$$r_c \leq R_{c,k}^{(n)}(\mathbf{F}), \forall k \in \mathcal{K} \quad (23d)$$

$$(13b), (13c)$$

2) *Lower-bound (LB) II:* We note that the lower bound approximation proposed in Lemma 1 is the first-order approximation of log function directly. Recall that each rate function is a composition function with an inner fractional SINR function embraced by an outer log function. Motivated by the convexity of the outer log function, another method is to approximate only the inner SINR function with its concave lower bound and keep the outer log function. Specifically, we introduce new variables $\gamma = [\gamma_1, \dots, \gamma_K]^T$ to denote the SINRs of the private streams at all users and variables $\gamma_c = [\gamma_{c,1}, \dots, \gamma_{c,K}]^T$ to denote the SINRs of the common streams at all users. Constraints (13d) and (13e) can be recast equivalently as

$$r_k \leq \log_2(1 + \gamma_k), \forall k \in \mathcal{K} \quad (24a)$$

$$r_c \leq \log_2(1 + \gamma_{c,k}), \forall k \in \mathcal{K} \quad (24b)$$

$$\gamma_k \leq \frac{|\mathbf{h}_k^H \mathbf{f}_k|^2}{r_{-k}}, \forall k \in \mathcal{K} \quad (24c)$$

$$\gamma_{c,k} \leq \frac{|\mathbf{h}_k^H \mathbf{f}_c|^2}{r_k}, \forall k \in \mathcal{K} \quad (24d)$$

where $r_{-k} = \sigma_k^2 + \sum_{i \in \mathcal{K} \setminus \{k\}} \mathbf{h}_k^H \mathbf{f}_i \mathbf{f}_i^H \mathbf{h}_k$ and $r_k = r_{-k} + \mathbf{h}_k^H \mathbf{f}_k \mathbf{f}_k^H \mathbf{h}_k$. The right hand side of (24c) and (24d) are all in the form of $\frac{x^2}{y}$. Thus, according to (14), we obtain (25) by applying substitutions $x = \mathbf{h}_k^H \mathbf{f}_k$ and $y = r_{-k}$, and (26) by applying substitutions $x = \mathbf{h}_k^H \mathbf{f}_c$ and $y = r_k$.

$$\frac{|\mathbf{h}_k^H \mathbf{f}_k|^2}{r_{-k}} \geq \frac{2\text{Re} \left\{ \mathbf{f}_k^{n,H} \mathbf{h}_k \mathbf{h}_k^H \mathbf{f}_k \right\}}{r_{-k}^n} - \left| \frac{\mathbf{h}_k^H \mathbf{f}_k^n}{r_{-k}^n} \right|^2 r_{-k} \triangleq \Gamma_k^{(n)}(\mathbf{F}), \quad (25)$$

$$\frac{|\mathbf{h}_k^H \mathbf{f}_c|^2}{r_k} \geq \frac{2\text{Re} \left\{ \mathbf{f}_c^{n,H} \mathbf{h}_k \mathbf{h}_k^H \mathbf{f}_c \right\}}{r_k^n} - \left| \frac{\mathbf{h}_k^H \mathbf{f}_c^n}{r_k^n} \right|^2 r_k \triangleq \Gamma_{c,k}^{(n)}(\mathbf{F}). \quad (26)$$

With (24a), (24b), and the concave lower bound approximations (25) and (26), Problem (13a) is reformulated equivalently as the following convex problem:

$$\max_{\mathbf{F} \in \mathcal{S}, \eta, \mathbf{r}, x, y, \gamma, \gamma_c} w\eta + \frac{(1-w)}{P_c} \sum_{i \in \mathcal{K}_c} r_i \quad (27a)$$

$$\text{s.t. } \gamma_k \leq \Gamma_k^{(n)}(\mathbf{F}), \forall k \in \mathcal{K} \quad (27b)$$

$$\gamma_{c,k} \leq \Gamma_{c,k}^{(n)}(\mathbf{F}), \forall k \in \mathcal{K} \quad (27c)$$

$$(13b), (13c), (23b), (24a), (24b).$$

Based on the specified LB I or LB II, the optimal SE-EE tradeoff problem can be achieved by designing \mathbf{f} under the SCA framework which is summarized in Algorithm 1. The initial points are generated as follows. $\mathbf{F}^{(0)}$ is created to meet the power constraint $\mathbf{F} \in \mathcal{S}$, and then $x^{(0)}$ and $y^{(0)}$ are obtained by setting constraints (12b) and (12c) to be equality, respectively.

Algorithm 1 SCA-based precoder design for the Problem (10)

Initialize: Set $n = 0$, and generate initialize points $(\mathbf{F}^{(n)}, x^{(n)}, y^{(n)})$.

- 1: **repeat**
- 2: Update $(\mathbf{F}^{(n+1)}, x^{(n+1)}, y^{(n+1)})$ according to (23) or (27).
- 3: $n = n + 1$.
- 4: **until** Convergence.

B. Convergence and Complexity Analysis

In this subsection, we discuss the convergence and per iteration complexity of Algorithm 1. To start with, the optimal solution obtained at the n -th iteration is also feasible for the Problem (23) and (27) at the next iteration [37]. Therefore, the sequence of the objective values generated by Algorithm 1 is non-decreasing and the sequence is bounded above due to the power constraints $\mathbf{F} \in \mathcal{S}$. Hence, the convergence of Algorithm 1 is guaranteed. Moreover, the proposed algorithm converges to a KKT solution of Problem (23) or (27) [37].

Next, we estimate the worst-case per-iteration complexity of Algorithm 1 with the SOCP (23) and general convex program (GCP) (27). Specifically, the computational complexity of solving SOCP is $\mathcal{O}(N_{\text{socp}}M_{\text{socp}}^{3.5} + N_{\text{socp}}^3M_{\text{socp}}^{2.5})$, where N_{socp} and M_{socp} are the dimension of second order cone and the number of second order cone constraints, respectively. Therefore, the per-iteration computational complexity of solving SOCP (23) is $\mathcal{O}(N_t(K+1)^{4.5} + N_t^3(K+1)^{5.5})$. Meanwhile, the per-iteration computational complexity of solving the GCP (27) is $\mathcal{O}(N_t^4(K+1)^4)$.

IV. WEIGHTED-POWER APPROACH

In the low transmit power constraint P_{\max} , both EE and SE increase with P_{\max} , and the optimal transmit power equals P_{\max} . Therefore, there is no conflict of interest between these two objective functions. However, when P_{\max} is large, the maximum SE is achieved when the optimal transmit power equals P_{\max} , which reduces the EE. In order to maximize EE, only part of the available power is used, which reduces the SE eventually. That means there is a tradeoff between EE and SE when the maximum available transmit power is high. Since both EE and SE are affected by transmit power, a weighted-power EE metric is proposed to investigate this tradeoff.

According to [18], maximizing EE and SE is also equivalent to minimizing their inverse. Therefore Problem (9) is equivalent to

$$\min_{\mathbf{F} \in \mathcal{S}} \left[\frac{g_{\text{RS}}(\mathbf{F})}{f_{\text{RS}}(\mathbf{F})}, \frac{1}{f_{\text{RS}}(\mathbf{F})} \right]. \quad (28)$$

Problem (28) is also solved via its corresponding single-objective problem as follows

$$\min_{\mathbf{F} \in \mathcal{S}} w \frac{g_{\text{RS}}(\mathbf{F})}{f_{\text{RS}}(\mathbf{F})} + (1-w) \frac{P_c}{f_{\text{RS}}(\mathbf{F})}, \quad (29)$$

where $w \in [0, 1]$. With the same denominator, Problem (29) is equivalent to

$$\max_{\mathbf{F} \in \mathcal{S}} \frac{f_{\text{RS}}(\mathbf{F})}{w(||\mathbf{F}||_F^2 + \chi f_{\text{RS}}(\mathbf{F})) + P_c}. \quad (30)$$

From a mathematical point of view, the metric in Problem (30) only has an additional constant w in the denominator compared with Problem (8). Hence, we name the objective of Problem (30) weighted-power EE metric. Physically speaking, by changing w from 0 to 1, we could investigate the SE-EE tradeoff. When $w = 0$, Problem (30) focuses only on maximizing the SE without considering how much energy is consumed. When w increases, it means there is a penalty for increasing the transmit power. This process may reduce the transmit power and thereby reduce the SE. When $w = 1$, Problem (30) focuses only on maximizing the EE.

Following the same method of obtaining Problem (23) and (27), Problem (30) can also be equivalently approximated by a SCA problem. Specifically, let a new variable $\hat{\eta}$ represent the weighted-power EE objective value in Problem (30) and take the place of η in the constraint (23b), i.e.,

$$\hat{\eta} \leq \phi^{(n)}(x, y). \quad (31)$$

Then constraint (13c) is also replaced by

$$w(||\mathbf{F}||_F^2 + \chi \sum_{i \in \mathcal{K}_c} r_i) + P_c \leq y. \quad (32)$$

In summary, Problem (30) can be approximated by LB I as an SOCP given by

$$\begin{aligned} & \max_{\mathbf{F} \in \mathcal{S}, \eta, \mathbf{r}, x, y} \hat{\eta} \\ & \text{s.t. } (13b), (23c), (23d), (31), (32), \end{aligned} \quad (33a)$$

or by using LB II as a GCP given by

$$\begin{aligned} & \max_{\mathbf{F} \in \mathcal{S}, \eta, \mathbf{r}, x, y, \gamma, \gamma_c} \hat{\eta} \\ & \text{s.t. } (13b), (24a), (24b), (27b), (27c), (31), (32). \end{aligned} \quad (34a)$$

Remark 1: Two different metrics are proposed to investigate the SE-EE tradeoff. The weighted-sum approach is very intuitive, because it directly studies the MOO problem (9) with EE metric and SE metric, and then solves the MOO problem through its corresponding SOO problem. The weighted-power approach is an indirect way. By controlling the proportion of power consumption in the denominator of the objective function in (30), we indirectly control the proportions of EE metric and SE metric in the original MOO problem (9).

Remark 2: SE Problem (6) and EE Problem (8) are special cases of SE-EE tradeoff Problem (10) and (30). In particular, when $w = 0$, Problem (10) and (30) reduce to Problem (6). When $w = 1$, Problem (10) and (30) boil down to Problem (8). Therefore, the proposed Algorithm 1 can be leveraged to solve individual SE and EE problems.

V. NUMERICAL RESULTS AND DISCUSSIONS

In this section, extensive numerical results are provided to evaluate the effectiveness of our proposed algorithm and the SE-EE tradeoff performance of RS. Without loss of generality, the BS is equipped with $N_t = 4$ transmit antennas, the noise power is $\sigma_k^2 = -20$ dBm, the static circuit power consumption is $P_c = 5$ dBW, $\chi = 0.1$ W/(bit/s/Hz), and the iterative procedure of all the algorithms considered in this section is terminated when the objective values between two subsequent iterations is less than 10^{-6} . The SNR in the figures is defined as $10 \log_{10}(P_{\max}/\sigma_k^2)$. Some specific simulation parameters are given according to different figures. According to [11], we consider the simplified geometric channel model as

$$\mathbf{h}_k = \nu_k [1, e^{j \frac{2\pi}{\lambda_c} d \cos \theta_k}, \dots, e^{j \frac{2\pi}{\lambda_c} (N_t - 1) d \cos \theta_k}]^T, \quad (35)$$

where ν_k is the gain of channel and characterizes channel disparity parameter, θ_k is the angle-of-departure (AoD) from BS to user k and characterizes the correlation between channels, and the scalar d is the interval of antennas and λ_c is the carrier wavelength. All algorithms are performed on a PC with a 1.99 GHz i7-8550U CPU and 16 GB RAM, and all convex problems are solved by using MOSEK solver [38].

A. Convergence Analysis

We note the fact that the computational complexity of Problem (23) and Problem (33) are the same, while that of Problem (27) and Problem (34) are also the same, hence this subsection only investigates the convergence performance of Problem (23) and Problem (27) proposed under weighted-sum approach.

Denote the proposed Algorithm 1 running with (23) and (27) as "RS-SOCP" and "RS-GCP", respectively. As a comparison, an SOCP approximation of Problem (27) has been considered by replacing the exponential cone (24a) and (24b) with their convex approximations (see (43) in [19]) and we denote this SOCP approximation method as "RS-GCP-SOCP". In addition, the Dinkelbach's algorithm proposed in [22] is also considered as our benchmark algorithm, which is denoted as "RS-D-MMSE". Basically, the idea of this benchmark algorithm is to use the WMMSE method to solve the parametric subproblems obtained from applying the Dinkelbach's algorithm to Problem (10). For completeness of the analysis, the NoRS is also considered, whose design problem can be solved by Dinkelbach's algorithm with semi-closed form solution [23] in each iteration or by (27) with minor modifications. Those methods are represented by "NoRS-D-bisearch" and "NoRS-GCP", respectively. The algorithms are summarized and compared in Table I.

Fig. 1 compares the numbers of iterations for those SCA algorithms with one layer iteration to converge when there are 3 users with $[\theta_1, \theta_2, \theta_3] = [0, \pi/9, 2\pi/9]$ and $\nu_1 = \nu_2 = \nu_3 = 1$. The SNR is 20 dB and the objective value in Y-axis is the optimal objective value of Problem (10). It is observed that the RS-GCP method takes the least number

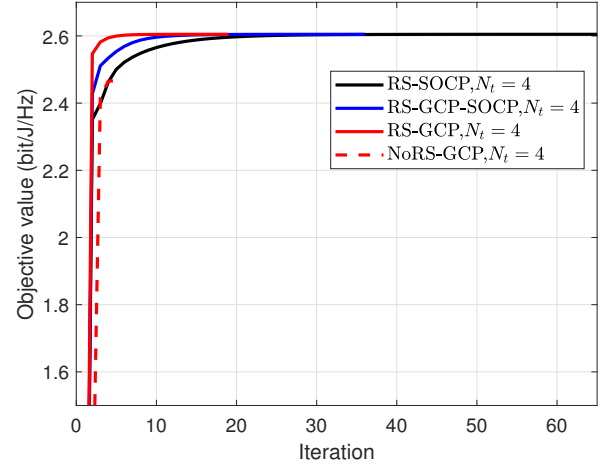


Fig. 1: Objective value versus number of iteration for RS/NoRS precoder designed by different SCA algorithms with SNR=20 dB, $N_t = 4$, $K = 3$ and $w = 0.5$.

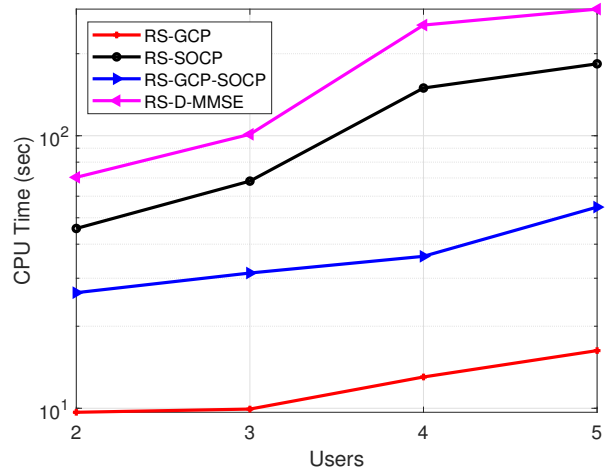


Fig. 2: CPU time versus K by applying different algorithms with SNR=20 dB, $N_t = 4$ and $w = 0.5$.

of iterations to converge since the GCP approximation is a tighter approximation of the original Problem (10). In contrast, the lower bound of rate proposed in Lemma 1, which is also known as the WMMSE lower bound, is a looser one.

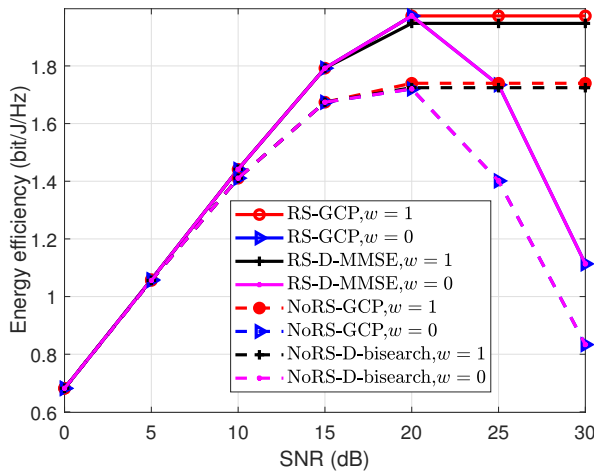
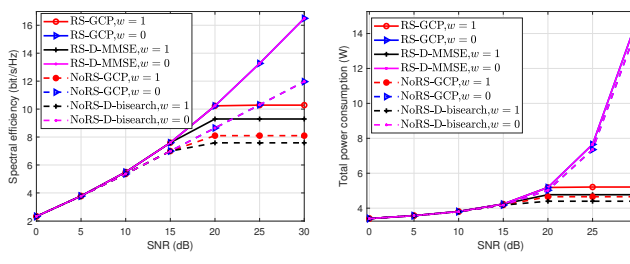
Fig. 2 then compares the overall CPU time of different algorithms when there are 5 users under random channel realizations with the entries following i.i.d. CSCG distribution. We note that the proposed RS-GCP has the lowest complexity among all algorithms used for RS optimization.

B. Energy Efficiency and Spectral Efficiency Performance of the RS Strategy

The SE and EE benefits of RS have been verified in [4]. Specifically, [4] separately investigates the SE maximization problem which is solved by the WMMSE method and EE

TABLE I: Comparison algorithm summary

	System model	Algorithm framework used to address the fractional programming	Method used in the inner iteration
RS-SOCP	RS	SCA	SOCP in (23)
RS-GCP	RS	SCA	GCP in (27)
RS-GCP-SOCP	RS	SCA	SOCP approximation [19] of GCP in (27)
RS-D-MMSE	RS	Dinkelbach's	WMMSE [22]
NoRS-D-bisearch	NoRS	Dinkelbach's	Semi-closed form solution with bisearch [23]
NoRS-GCP	NoRS	SCA	GCP in (27) with $\ \mathbf{f}_c\ ^2 = 0$

Fig. 3: Energy efficient SNR for RS/NoRS precoder designed with $N_t = 4$ and $K = 2$.Fig. 4: Spectral efficiency and power consumption versus SNR for RS/NoRS precoder designed with $N_t = 4$ and $K = 2$.

maximization problem which is solved by the SCA method. However, how the system EE of RS changes with the SNR, and how RS can control its SE and power consumption to achieve high EE, have never been studied. In this subsection, we compare the EE of RS with that of NoRS as SNR increases as well as the corresponding SE and power consumption achieved with both strategies. As we mentioned in Remark 2, Algorithm 1 can be directly adopted to solve the SE maximization Problem (6) and the EE maximization Problem (8) by setting $w = 0$ and $w = 1$, respectively.

Fig. 3 shows the EE comparison in different schemes containing 2 users with AoDs $[\theta_1, \theta_2] = [0, \pi/9]$. We should

notice that when $w = 0$, the value of EE is the ratio of the optimal SE over the power consumption. For the sake of argument, the corresponding denominators and numerators of EE, i.e., achievable SE and achievable transmit power consumption, are also shown in Fig. 4(a) and Fig. 4(b), respectively. *Firstly*, the EE performance of SCA algorithms and their corresponding Dinkelbach's algorithms are almost the same in both RS and NoRS strategies. *Secondly*, the EE of each algorithm with $w = 1$ is equal to that with $w = 0$ at low SNR, while at high SNR their behaviors conflict with each other. This is because the aim of Problem (8) is to optimize EE and keep the objective value non-decrease, while that of Problem (6) is to use all the available transmit power to produce maximum SE and even sacrifice EE. *Thirdly*, the EE produced by RS precoder is higher than that generated by NoRS precoder. This behavior is easy to understand in the class of ' $w = 0$ ' curves, where RS precoder uses the same available power (see Fig. 4(b)) to produce higher achievable SE (see Fig. 4(a)). While in the class of ' $w = 1$ ' curves, RS precoder uses a little bit higher power (see Fig. 4(b)) to produce much higher SE (see Fig. 4(a)) than NoRS precoder, the resulting EE value of RS precoder naturally much higher than that of NoRS precoder. That is to say RS strategy shows its crucial benefits in EE communication system. Finally, the behavior of these curves with $w = 1$ in Fig. 4(a) and Fig. 4(b) reveals the performance superiority of SCA algorithm over Dinkelbach's algorithm. Basically, while achieving the same high EE, the SE resulted by SCA algorithm is higher than that generated by Dinkelbach's algorithm, which guarantees the quality of service (QoS) of the communication systems.

C. The SE-EE Tradeoff of the RS Strategy

This subsection investigates the SE-EE tradeoff performance of the RS and NoRS strategies where the RS/NoRS precoders are designed by the GCP since it generates better objective values and incurs the least CPU time.

Fig. 5 shows the SE-EE tradeoff generated by our proposed weighted-sum approach (10) and weighted-power approach (30) when $K = 2$ and $[\theta_1, \theta_2] = [0, \pi/9]$. *Firstly*, it is obvious that the performances of the weighted-sum and weighted-power approaches are the same. While the mathematical model of the weighted-power metric is more concise than the weighted-sum metric. *Secondly*, when SNR=15 dB, the EE and SE remain unchanged in the range of w from 0 to 1, which indicates that the interests between EE and SE do not conflict with each other at low SNR.

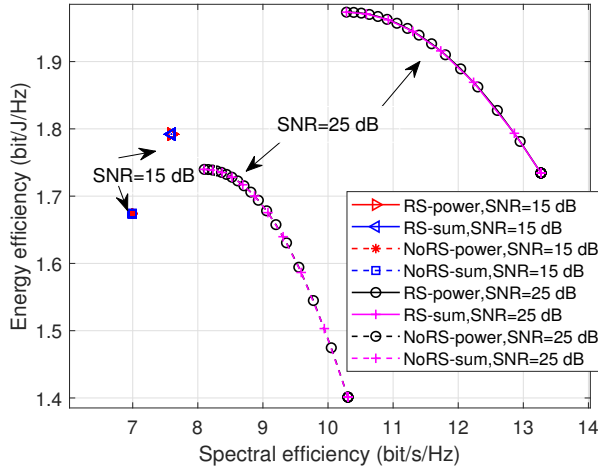


Fig. 5: The SE-EE tradeoff for RS/NoRS precoder designed by different approaches with $N_t = 4$, $K = 2$ and $\chi = 0.1$ W/(bit/s/Hz).

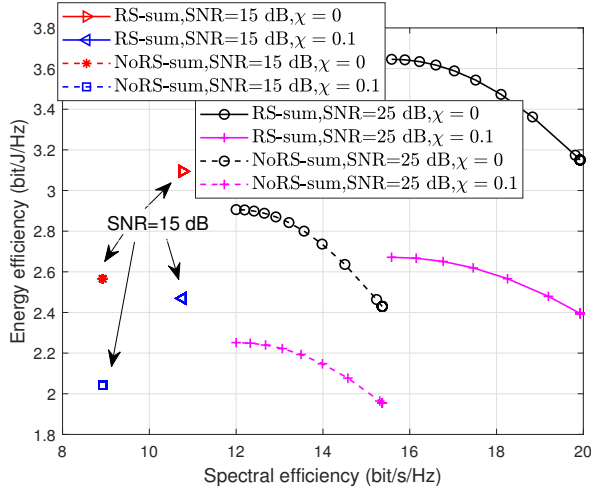


Fig. 6: The SE-EE tradeoff for RS/NoRS precoder with $N_t = 4$ and $K = 4$.

Finally, when SNR=25 dB, we noticed a tradeoff between EE and SE. Since the performance of the weighted-sum approach and the weighted-power approach is the same, the following simulations only adopt the weighted-sum approach to investigate the SE-EE tradeoff performance.

Fig. 6 considers the 4-user case with $[\theta_1, \theta_2, \theta_3, \theta_4] = [0, \pi/9, 2\pi/9, 3\pi/9]$ at different SNR and χ . It is observed that the EE decreases with the increase of χ , but the change of χ does not affect the SE.

Fig. 7 shows the SE-EE tradeoff performance with different $\theta_2 = \{\pi/18, \pi/9, \pi/6\}$. It is obvious that the AoDs has no effect on the performance of the NoRS strategy, but has a significant effect on the performance of the RS strategy. This is because when users' channels are aligned (e.g., $\theta_2 = \{\pi/18, \pi/9\}$) and the inter-channel interference is large, RS strategy can perform more effective interference

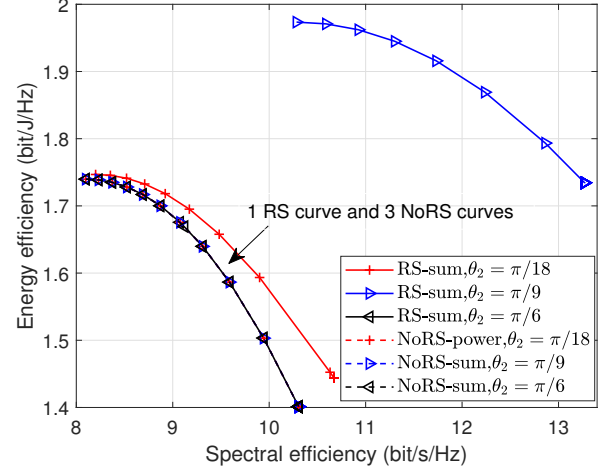


Fig. 7: The SE-EE tradeoff for RS/NoRS precoder with SNR=25 dB, $N_t = 4$, $K = 2$ and $\chi = 0.1$ W/(bit/s/Hz).

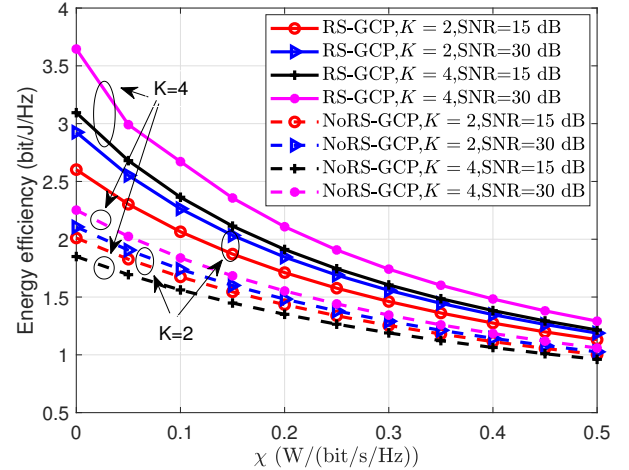


Fig. 8: Energy efficiency versus χ with $N_t = 4$, $K = 2$ and $w = 1$.

management than NoRS strategy. When users' channels are nearly orthogonal (e.g., $\theta_2 = \pi/6$), the interference management advantage of the RS strategy becomes not obvious. Finally, it is found that the RS strategy performs better than the NoRS strategy when the SE metric occupies a large proportion of the multi-objective optimization problem. That is to say the performance gain of RS in terms of spectral efficiency is more obvious than that of energy efficiency.

Following the conclusion obtained from Fig. 5 that χ does not affect the SE, Fig. 8 only depicts the effect of rate-dependent dynamic circuit power consumption on EE performance when $w = 1$. It shows that the increment of χ leads to the decrease of the EE.

Fig. 9 illustrates the effect of K on the SE-EE tradeoff with RS and NoRS under CSCG random channels. The average trade-off regions of different strategies are generated over 200 random channel realizations when SNR=25 dB

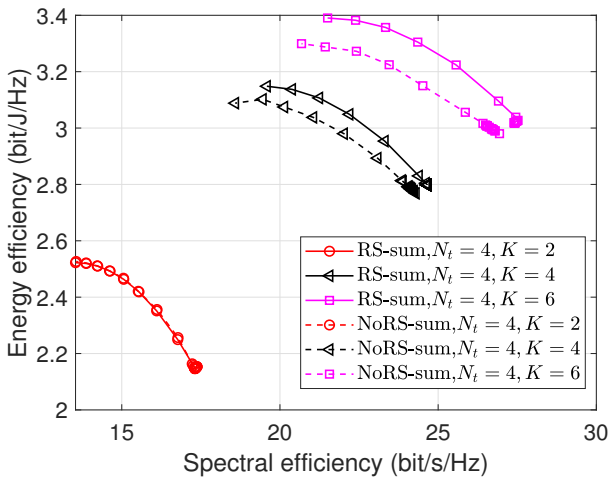


Fig. 9: The SE-EE tradeoff for RS/NoRS precoder with SNR=25 dB and $\chi = 0.1\text{W}/(\text{bit/s/Hz})$.

and $\chi = 0.1\text{W}/(\text{bit/s/Hz})$. It is observed that the EE-SE trade-off region gap between RS and NoRS increases as the number of user increases. This shows that the interference management advantage of RS over NoRS is more obvious in the overloaded scenario.

VI. CONCLUSION

In this paper, we have addressed the SE-EE tradeoff of RSMA in a multi-antenna Broadcast Channel and have shown the potential of RSMA to boost the SE-EE tradeoff. The tradeoff problem is a multiple-objective optimization problem and each objective function is non-convex due to the complex sum rate expressions and power consumption expression. In order to overcome those challenges, we firstly proposed two approaches, namely weighted-sum approach and weighted-power approach, to obtain the equivalent single objective optimization problems. Then SCA algorithm is used to get the optimal precoder. Numerical results demonstrate the effectiveness of the proposed algorithm. More importantly, compared to the conventional non-RS strategy, RS has significant performance gains in terms of EE and SE.

APPENDIX A PROOF OF LEMMA 1

Proof: We first derive the concave lower bound function (15) of common rate R_k , and then (19) could be derived following the same procedure directly. For the convenience of deduction, (4) needs to be reformulated in a more readable equivalent, as

$$\begin{aligned} R_k &= \log_2 \left(1 + \frac{\mathbf{h}_k^H \mathbf{f}_k \mathbf{f}_k^H \mathbf{h}_k}{\sigma_k^2 + \sum_{i \in \mathcal{K} \setminus \{k\}} \mathbf{h}_k^H \mathbf{f}_i \mathbf{f}_i^H \mathbf{h}_k} \right) \\ &= \log_2 \left(1 + r_{-k}^{-1} \mathbf{f}_k^H \mathbf{h}_k \mathbf{h}_k^H \mathbf{f}_k \right) \\ &= -\log_2 \left(1 - r_k^{-1} \mathbf{f}_k^H \mathbf{h}_k \mathbf{h}_k^H \mathbf{f}_k \right) \end{aligned} \quad (36)$$

where $r_{-k} = \sigma_k^2 + \sum_{i \in \mathcal{K} \setminus \{k\}} \mathbf{h}_k^H \mathbf{f}_i \mathbf{f}_i^H \mathbf{h}_k$ and $r_k = r_{-k} + \mathbf{h}_k^H \mathbf{f}_k \mathbf{f}_k^H \mathbf{h}_k$. The third equation of (36) follows from applying the Woodbury matrix identity [39]. Let $R_k(\mathbf{f}_k, r_k)$ represent the third equation of (36) with constraint $r_k = \sigma_k^2 + \sum_{i \in \mathcal{K}} \mathbf{h}_k^H \mathbf{f}_i \mathbf{f}_i^H \mathbf{h}_k$, $-\log_2(\cdot)$ is convex and $1 - r_k^{-1} \mathbf{f}_k^H \mathbf{h}_k \mathbf{h}_k^H \mathbf{f}_k$ is jointly concave in (\mathbf{f}_k, r_k) , thus $R_k(\mathbf{f}_k, r_k)$ is jointly convex in (\mathbf{f}_k, r_k) [35] and minorized by its first-order approximation at fixed point (\mathbf{f}_k^n, r_k^n) . Specifically,

$$\begin{aligned} R_k(\mathbf{f}_k, r_k) &\geq R_k(\mathbf{f}_k^n, r_k^n) + \left(\frac{\partial R_k}{\partial \mathbf{f}_k} \Big|_{\mathbf{f}_k=\mathbf{f}_k^n} \right)^T (\mathbf{f}_k - \mathbf{f}_k^n) \\ &\quad + \left(\frac{\partial R_k}{\partial \mathbf{f}_k^*} \Big|_{\mathbf{f}_k^*=\mathbf{f}_k^{n,*}} \right)^T (\mathbf{f}_k^* - \mathbf{f}_k^{n,*}) + \frac{\partial R_k}{\partial r_k} \Big|_{r_k=r_k^n} (r_k - r_k^n) \\ &= R_k(\mathbf{f}_k^n, r_k^n) + 2\text{Re} \{ a_k \mathbf{b}_k^H (\mathbf{f}_k - \mathbf{f}_k^n) \} \\ &\quad - a_k(r_k^n)^{-2} \mathbf{f}_k^{n,H} \mathbf{h}_k \mathbf{h}_k^H \mathbf{f}_k^n (r_k - r_k^n), \end{aligned} \quad (37)$$

where a_k and \mathbf{b}_k are defined in (16) and (17), respectively. Undo $r_k = \sigma_k^2 + \sum_{i \in \mathcal{K}} \mathbf{h}_k^H \mathbf{f}_i \mathbf{f}_i^H \mathbf{h}_k$ and $r_k^n = \sigma_k^2 + \sum_{i \in \mathcal{K}} \mathbf{h}_k^H \mathbf{f}_i^n \mathbf{f}_i^{n,H} \mathbf{h}_k$, the last equation of (37) equals (15).

APPENDIX B PROOF OF LEMMA 2

Proof: We first show the lower bound of rate R_k derived via MMSE. The lower bound of the matrix version in MIMO system can be found in [36]. Then we proof that the lower bound obtained via MMSE is the same with (15).

1) *lower bound obtained via MMSE:* Let w_k be the equalizer of user k for private stream. Then MSE of estimated signal $\hat{s}_k = w_k^H y_k$ is given by

$$\begin{aligned} e_k &= w_k^* (\sigma_k^2 + \sum_{i \in \mathcal{K}} \mathbf{h}_k^H \mathbf{f}_i \mathbf{f}_i^H \mathbf{h}_k) w_k - 2\text{Re} \{ w_k^* \mathbf{h}_k^H \mathbf{f}_k \} + 1 \\ &= r_k |w_k|^2 - 2\text{Re} \{ w_k^* \mathbf{h}_k^H \mathbf{f}_k \} + 1. \end{aligned} \quad (38)$$

(36) is rewritten as

$$R_k(q_k) = -\log_2(q_k) \quad (39)$$

where $q_k = 1 - r_k^{-1} \mathbf{f}_k^H \mathbf{h}_k \mathbf{h}_k^H \mathbf{f}_k$. R_k is a convex function of q_k and minorized by its linear approximation as

$$\begin{aligned} R_k(q_k) &= -\log_2(q_k) \\ &\geq -\log_2(q_k^n) - (q_k - q_k^n)/q_k^n \\ &= -\log_2(q_k^n) + 1 - q_k/q_k^n \end{aligned} \quad (40)$$

at fixed point q_k^n . In addition, e_k/q_k^n is a convex function of w_k and the global minimum is achieved at MMSE receiver, i.e.,

$$w_k^{opt} = \mathbf{h}_k^H \mathbf{f}_k / r_k \quad (41)$$

Put (41) into (38), one has

$$e_k(w_k^{opt}) = q_k. \quad (42)$$

Therefore

$$q_k/q_k^n \leq e_k/q_k^n \quad (43)$$

for any w_k . And furthermore

$$\begin{aligned} R_k &\geq -\log_2(q_k^n) + 1 - q_k/q_k^n \\ &\geq -\log_2(q_k^n) + 1 - e_k/q_k^n. \end{aligned} \quad (44)$$

Keep in mind that (41) is obtained based on given \mathbf{f} . In Alternating Iterative Algorithm, denote \mathbf{f}^n as the optimal precoders at the n -th iteration, then the optimal equalizer at the $(n+1)$ -th iteration is

$$w_k^{n+1} = \mathbf{h}_k^H \mathbf{f}_k^n / r_k^{n+1} \quad (45)$$

Put (45) into e_k/q_k^n as

$$\begin{aligned} e_k/q_k^n &= \left(r_k |w_k^{n+1}|^2 - w_k^{n+1,*} \mathbf{h}_k^H \mathbf{f}_k - \mathbf{f}_k^H \mathbf{h}_k w_k^{n+1} + 1 \right) / q_k^n \\ &= \sum_{i \in \mathcal{K}} \mathbf{h}_k^H \mathbf{f}_i \mathbf{f}_i^H \mathbf{h}_k |w_k^{n+1}|^2 / q_k^n + 1/q_k^n \\ &\quad - 2\operatorname{Re} \left\{ w_k^{n+1,*} \mathbf{h}_k^H \mathbf{f}_k / q_k^n \right\} + \sigma_k^2 |w_k^{n+1}|^2 / q_k^n \end{aligned} \quad (46)$$

Therefore (44) is

$$\begin{aligned} R_k &\geq -\log_2(q_k^n) + 1 - e_k/q_k^n \\ &= -\log_2(q_k^n) + 1 - \sum_{i \in \mathcal{K}} \mathbf{h}_k^H \mathbf{f}_i \mathbf{f}_i^H \mathbf{h}_k |w_k^{n+1}|^2 / q_k^n \\ &\quad + 2\operatorname{Re} \left\{ w_k^{n+1,*} \mathbf{h}_k^H \mathbf{f}_k / q_k^n \right\} - \sigma_k^2 |w_k^{n+1}|^2 / q_k^n - 1/q_k^n \\ &= \text{const} + 2\operatorname{Re} \left\{ w_k^{n+1,*} \mathbf{h}_k^H \mathbf{f}_k / q_k^n \right\} \\ &\quad - \sum_{i \in \mathcal{K}} \mathbf{h}_k^H \mathbf{f}_i \mathbf{f}_i^H \mathbf{h}_k |w_k^{n+1}|^2 / q_k^n \end{aligned} \quad (47)$$

where

$$\text{const}_{\text{mmse},k} = -\log_2(q_k^n) + 1 - \sigma_k^2 |w_k^{n+1}|^2 / q_k^n - 1/q_k^n \quad (48)$$

The equation of (47) holds when $\mathbf{f} = \mathbf{f}^n$.

2) *Claim the Equivalence:* In the following, we claim that the last equation of (47) equals (15).

In particular,

$$\begin{aligned} a_k &= 1/q_k^n, \\ \mathbf{b}_k &= \mathbf{h}_k w_k^{n+1}. \end{aligned}$$

The constant in (48) equals that in (18), i.e.,

$$\begin{aligned} &\text{const}_k \\ &= R_k(\mathbf{f}^n) - 2\operatorname{Re} \left\{ a_k \mathbf{b}_k^H \mathbf{f}_k^n \right\} + a_k \sum_{i \in \mathcal{K}} \mathbf{f}_i^{n,H} \mathbf{b}_k \mathbf{b}_k^H \mathbf{f}_i^n \\ &= R_k(\mathbf{f}^n) - 2\operatorname{Re} \left\{ a_k \mathbf{b}_k^H \mathbf{f}_k^n \right\} \\ &\quad + \left(\mathbf{h}_k^H \sum_{i \in \mathcal{K}} \mathbf{f}_i^n \mathbf{f}_i^{n,H} \mathbf{h}_k + \sigma_k^2 \right) a_k |w_k^{n+1}|^2 - \sigma_k^2 a_k |w_k^{n+1}|^2 \\ &= R_k(\mathbf{f}^n) - 2\operatorname{Re} \left\{ a_k \mathbf{b}_k^H \mathbf{f}_k^n \right\} \\ &\quad + r_k^n a_k |w_k^{n+1}|^2 - \sigma_k^2 a_k |w_k^{n+1}|^2 \\ &= R_k(\mathbf{f}^n) - \sigma_k^2 a_k |w_k^{n+1}|^2 - a_k \mathbf{b}_k^H \mathbf{f}_k^n \\ &= R_k(\mathbf{f}^n) - \sigma_k^2 a_k |w_k^{n+1}|^2 + (a_k - a_k \mathbf{b}_k^H \mathbf{f}_k^n - a_k) \\ &= R_k(\mathbf{f}^n) - \sigma_k^2 a_k |w_k^{n+1}|^2 + (a_k(1 - \mathbf{b}_k^H \mathbf{f}_k^n) - a_k) \\ &= R_k(\mathbf{f}^n) - \sigma_k^2 a_k |w_k^{n+1}|^2 + 1 - a_k \\ &= \text{const}_{\text{mmse},k} \end{aligned} \quad (49)$$

The penultimate equation is because $a_k = 1/(1 - \mathbf{b}_k^H \mathbf{f}_k^n)$.

REFERENCES

- [1] Te Han and K. Kobayashi, "A new achievable rate region for the interference channel," *IEEE Trans. Inf. Theory*, vol. 27, no. 1, pp. 49–60, Jan. 1981.
- [2] B. Clerckx, H. Joudeh, C. Hao, M. Dai, and B. Rassouli, "Rate splitting for MIMO wireless networks: A promising PHY-layer strategy for LTE evolution," *IEEE Commun. Mag.*, vol. 54, no. 5, pp. 98–105, May 2016.
- [3] B. Clerckx, Y. Mao, R. Schober, and H. Poor, "Rate-splitting unifying SDMA, OMA, NOMA, and multicasting in MISO broadcast channel: A simple two-user rate analysis," [*Online*] <https://arxiv.org/abs/1906.04474>, 2019.
- [4] Y. Mao, B. Clerckx, and V. O. K. Li, "Rate-splitting for multi-antenna non-orthogonal unicast and multicast transmission: Spectral and energy efficiency analysis," *IEEE Trans. Commun.*, pp. 1–1, Sep. 2019.
- [5] Y. Mao, B. Clerckx, and V. O. Li, "Rate-splitting multiple access for downlink communication systems: Bridging, generalizing, and outperforming SDMA and NOMA," *EURASIP J. Wireless Commun. Netw.*, vol. 2018, no. 1, p. 133, May 2018.
- [6] A. Alameer Ahmad, H. Dahrouj, A. Chaaban, A. Sezgin, and M. Alouini, "Interference mitigation via rate-splitting and common message decoding in cloud radio access networks," *IEEE Access*, vol. 7, pp. 80350–80365, Jun. 2019.
- [7] Y. Mao, B. Clerckx, and V. O. K. Li, "Rate-splitting multiple access for coordinated multi-point joint transmission," in *Proc. IEEE Int. Conf. Commun. (ICC Workshops)*, May 2019, pp. 1–6.
- [8] Z. Yang, M. Chen, W. Saad, and M. Shikh-Bahaei, "Optimization of Rate Allocation and Power Control for Rate Splitting Multiple Access (RSMA)," 2019. [*Online*]. Available: <https://arxiv.org/abs/1903.08068>
- [9] C. Hao, Y. Wu, and B. Clerckx, "Rate analysis of two-receiver MISO broadcast channel with finite rate feedback: A rate-splitting approach," *IEEE Trans. Commun.*, vol. 63, no. 9, pp. 3232–3246, Sep. 2015.
- [10] M. Dai, B. Clerckx, D. Gesbert, and G. Caire, "A rate splitting strategy for massive MIMO with imperfect CSIT," *IEEE Trans. Wireless Commun.*, vol. 15, no. 7, pp. 4611–4624, Jul. 2016.
- [11] M. Dai and B. Clerckx, "Multiuser millimeter wave beamforming strategies with quantized and statistical CSIT," *IEEE Trans. Wireless Commun.*, vol. 16, no. 11, pp. 7025–7038, Nov. 2017.
- [12] H. Joudeh and B. Clerckx, "Robust transmission in downlink multiuser MISO systems: A rate-splitting approach," *IEEE Trans. Signal Process.*, vol. 64, no. 23, pp. 6227–6242, Dec. 2016.
- [13] ———, "Sum-rate maximization for linearly precoded downlink multiuser MISO systems with partial CSIT: A rate-splitting approach," *IEEE Trans. Commun.*, vol. 64, no. 11, pp. 4847–4861, Nov. 2016.
- [14] ———, "Rate-splitting for max-min fair multigroup multicast beamforming in overloaded systems," *IEEE Trans. Wireless Commun.*, vol. 16, no. 11, pp. 7276–7289, Nov. 2017.

[15] J. Zhang, B. Clerckx, J. Ge, and Y. Mao, "Cooperative rate-splitting for MISO broadcast channel with user relaying, and performance benefits over cooperative NOMA," *IEEE Signal Process. Lett.*, pp. 1–1, 2019.

[16] Y. Mao, B. Clerckx, and V. O. K. Li, "Energy efficiency of rate-splitting multiple access, and performance benefits over SDMA and NOMA," *Proc. IEEE Int. Symp. Wireless Commun. Syst. (ISWCS)*, 2018.

[17] Y. Chen, S. Zhang, S. Xu, and G. Y. Li, "Fundamental trade-offs on green wireless networks," *IEEE Commun. Mag.*, vol. 49, no. 6, pp. 30–37, June 2011.

[18] O. Amin, E. Bedeer, M. H. Ahmed, and O. A. Dobre, "Energy efficiency-spectral efficiency tradeoff: A multiobjective optimization approach," *IEEE Trans. Veh. Technol.*, vol. 65, no. 4, pp. 1975–1981, Apr. 2016.

[19] O. Tervo, L. Tran, H. Pennanen, S. Chatzinotas, B. Ottersten, and M. Juntti, "Energy-efficient multicell multigroup multicasting with joint beamforming and antenna selection," *IEEE Trans. Signal Process.*, vol. 66, no. 18, pp. 4904–4919, Sep. 2018.

[20] R. Zhang, Y. Li, C. Wang, Y. Ruan, Y. Fu, and H. Zhang, "Energy-spectral efficiency trade-off in underlaying mobile D2D communications: An economic efficiency perspective," *IEEE Trans. Wireless Commun.*, vol. 17, no. 7, pp. 4288–4301, Jul. 2018.

[21] W. Dinkelbach, "On nonlinear fractional programming," *Manage. Sci.*, vol. 13, no. 7, pp. 492–498, 1967.

[22] S. He, Y. Huang, S. Jin, F. Yu, and L. Yang, "Max-min Energy efficient beamforming for multicell multiuser joint transmission systems," *IEEE Commun. Lett.*, vol. 17, no. 10, pp. 1956–1959, Oct. 2013.

[23] M. Razaviyayn, *Successive convex approximation: Analysis and applications*. Ph.D. dissertation, Univ. Minnesota, Minneapolis, MN, USA, 2001.

[24] O. Tervo, L. Tran, and M. Juntti, "Optimal energy-efficient transmit beamforming for multi-user MISO downlink," *IEEE Trans. Signal Process.*, vol. 63, pp. 5574–5588, Jul. 2015.

[25] K. Nguyen, Q. Vu, L. Tran, and M. Juntti, "Energy efficiency fairness for multi-pair wireless-powered relaying systems," *IEEE J. Select. Areas Commun.*, vol. 37, no. 2, pp. 357–373, Feb. 2019.

[26] G. Caire and S. Shamai, "On the achievable throughput of a multiantenna Gaussian broadcast channel," *IEEE Trans. Inform. Theory*, vol. 49, no. 7, pp. 1691–1706, Jul. 2003.

[27] S. S. Christensen, R. Agarwal, E. D. Carvalho, and J. M. Cioffi, "Weighted sum-rate maximization using weighted MMSE for MIMO-BC beamforming design," *IEEE Trans. Wireless Commun.*, vol. 7, no. 12, pp. 4792–4799, Dec. 2008.

[28] C. Pan, W. Xu, J. Wang, H. Ren, W. Zhang, N. Huang, and M. Chen, "Pricing-based distributed energy-efficient beamforming for MISO interference channels," *IEEE J. Select. Areas Commun.*, vol. 34, no. 4, pp. 710–722, Apr. 2016.

[29] A. Zappone, E. Björnson, L. Sanguinetti, and E. A. Jorswieck, "Globally optimal energy-efficient power control and receiver design in wireless networks," *IEEE Trans. Signal Process.*, vol. 65, no. 11, Jun. 2017.

[30] B. Matthiesen, C. Hellings, and E. A. Jorswieck, "Energy efficiency: Rate splitting vs. point-to-point codes in gaussian interference channels," in *Proc. SPAWC*, Jul. 2019, pp. 1–5.

[31] E. Björnson, L. Sanguinetti, J. Hoydis, and M. Debbah, "Optimal design of energy-efficient multi-user MIMO systems: Is massive MIMO the answer?" *IEEE Trans. Wireless Commun.*, vol. 14, no. 6, pp. 3059–3075, Jun. 2015.

[32] K. Xiong, P. Fan, Y. Lu, and K. B. Letaief, "Energy efficiency with proportional rate fairness in multirelay OFDM networks," *IEEE J. Select. Areas Commun.*, vol. 34, no. 5, pp. 1431–1447, May 2016.

[33] C. Isheden and G. P. Fettweis, "Energy-efficient multi-carrier link adaptation with sum rate-dependent circuit power," in *Proc. IEEE Glob. Commun. Conf. (GLOBECOM)*, Dec. 2010, pp. 1–6.

[34] Y. Yang, M. Pesavento, S. Chatzinotas, and B. Ottersten, "Energy efficiency optimization in MIMO interference channels: A successive pseudoconvex approximation approach," *IEEE Trans. Signal Process.*, vol. 67, no. 15, pp. 4107–4121, Aug. 2019.

[35] S. Boyd and L. Vandenberghe, *Convex optimization*. Cambridge Univ. Press, 2004.

[36] A. Lu, X. Gao, W. Zhong, C. Xiao, and X. Meng, "Robust transmission for massive MIMO downlink with imperfect CSI," *IEEE Trans. Commun.*, vol. 67, no. 8, pp. 5362–5376, Aug. 2019.

[37] B. R. Marks and G. P. Wright, "A general inner approximation algorithm for nonconvex mathematical programs," *Oper. Res.*, vol. 26, no. 4, pp. 681–683, Jul.-Aug. 1978.

[38] "The mosek optimization toolbox for MATLAB manual." *Version 7.1 (revision 28)*. [Online] <http://mosek.com>, accessed on: Mar. 20, 2015.

[39] N. Higham, *Accuracy and stability of numerical algorithms* (2nd ed.). SIAM, 2002.